Cellular Indoor OWC Systems with an optimal Lambertian Order and a Handover Algorithm

[1]Dehao.Wu, [2]Z. Ghassemlooy, [1]Wen-de Zhong and [1]Chen Chen

[1]School of Electrical and Electronic Engineering, Nanyang Technological University,
50 Nanyang Avenue, Singapore 639798.
E-mail: dehao.wu@ntu.edu.sg Optical Communications Research Group, NCRLab, Faculty of Engineering and Environment,
[2]Northumbria University, Newcastle Upon Tyne, UK.
E-mail: z.ghassemlooy@northumbria.ac.uk

***Abstract*— In recent years, optical wireless communication (OWC) has been presented as a viable and promising technology to achieve a high-speed indoor wireless link. In this paper, to fully exploit the advantages of OWC, an optimal Lambertian order (OLO) and a handover algorithm are proposed and adopted for a cellular indoor OWC system to further extend the transmission bandwidth. We firstly describe these two techniques for a cellular configuration. Then, the channel characteristics including the optical power distribution and the RMS delay spread for a four-cell structure are simulated and analyzed. The results show that with an OLO and a handover algorithm applied on the link, the transmission bandwidth of the system can be extended by almost ten times compared to the non-optimized scenario. However, the improvement contributed by the handover algorithm depends on the numbers of the cells and the locations of the users as well.**

Keywords—Optical wireless communication (OWC), Cellular configruation, Optimal Lambertian order, Handover and transmission bandwidth.

I. INTRODUCTION

With the emergence of portable information terminals at work and at home, the demand for high bit rate wireless service over a short range in local area networks (LANs) is continuously increasing. There are a number of RF technologies that are currently being used to offer broadband wireless communications [1-3]. The IEEE 802.11 a/b/g WiFi technologies are widely exploited in commercial products due to their low cost, technological maturity, and high product penetration [4, 5]. However, the maximum transmission data rate is limited to ~ 100 Mb/s. Recently, with the rapid growth of internet users, file and video sharing, audio and video broadcasting, the rapid growth of the bandwidth requirement by the end-users has placed a huge pressure on already congested RF systems. To overcome this bandwidth bottleneck, the OWC technology has shown the potential to achieve both high spatial coverage and high bit rates transmission for the indoor wireless communications. On the other hand, as a complementary technology to RF, indoor OWC systems offer a number of advantages such as inherent unregulated bandwidth, low-cost, inherent immunity to the electromagnetic interference, the possibility of wavelength reuse and security at the physical layer [6]. Therefore, due to its high degree of privacy and security, such systems are the ideal solutions for military use or financial transactions.

The visible light communication (VLC) system incorporated with white LEDs lighting has attracted considerable attention over the past decade. [7, 8]. The illumination of an VLC system is generally restricted to 300 to 1500 lx based on the International Organization for Standardization (ISO) standard [9]. This minimal illumination level at visible spectrum (~ 300 lx) offers a higher signal-to-noise ratio (SNR), which is >50 dB in indoor OWC systems [10]. Therefore, the indoor OWC access technology employing LEDs becomes a possible and economical solution to overcome the current bandwidth congestion problem for the indoor wireless access networks. However, the main challenge for VLC providing a high data rate transmission is the slow modulation bandwidth of the commercial white LEDs, which is typically a few megahertz. Fortunately, with the development of the technology, LED with a large modulation bandwidth is being designed and fabricated. In [11], a LED with a diameter of 50 μm (μLED) is introduced, which provides a 3-dB modulation bandwidth of at least 60 MHz. There is no doubt that in the near future, LED with a higher modulation bandwidth will commercially available. In this paper, our theoretical work focuses on the OWC technology which provides a bit rate of more than 100 Mb/s for a single channel.

Another very important issue for an indoor OWC system is the multipath induced intersymbol interference (ISI), which would significantly limit the maximum transmission data rate of the system [12-14]. Due to the physical properties of an indoor environment, the reflection from the ceiling, wall and other objectives always exist for an indoor OWC system. In addition, for a system employing multiple transmitters, the ISI caused by neighbour transmitters is too significant to ignore [15]. Therefore, it is necessary to study this challenge and mitigate the negative effects. Analysis of the multipath time dispersion for an indoor OWC channel has been studied in [16, 17]. It is shown that lower multipath distortion can be achieved by optimizing the divergence angle of the LED and by employing a special configuration [17]. A more uniform power distribution is proposed in [18, 19] where a reduced ISI has been achieved by using a holographic diffuser. In [20], spotlight scheme has been proposed for the high data rate transmission and the results

978-1-4799-5359-2/14/$31.00 ©2014 IEEE

show that indoor OWC links employing LEDs with small divergence angles have lower channel distortion than those with large divergence angles. Therefore, an OWC system with a multi-cell configuration is proposed as a preferred solution to achieve a higher transmission bandwidth. However, in the previous studies, little attention has been given to optimize the divergence angles of LEDs and its impact on the time dispersion and the channel transmission bandwidth. In this paper, we propose optimum divergence angles of LEDs for a 4-cell configuration to achieve its optimal transmission bandwidth. Additionally, taking the numbers of users and their locations into account, a handover scheme is adopted in this system which further extends the channel transmission bandwidth to its best performance.

This paper is organized as follows: the system configuration and OWC channel characteristics are described in Section II. In Section III, the OLO of the LEDs and a handover algorithm are introduced. Then, the simulation results and discussion are outlined in Section IV. Finally, conclusions are given in section V.

II. System Description

A. System configuration

Fig. 1 shows the proposed indoor OWC link with multiple cells configuration. The room has a dimension of 5×5×3 m^3 (length, width, height) which is divided into i equal sections (cells). Each cell employs a group of LEDs mounted at the room ceiling, which is marked as S_i in Fig. 1. At the receiving plane, the optical footprint has its maximum and minimum intensities at the center and the edge of the cell, respectively. Cells have the same beam profile and the overall footprint covers the whole floor of the room. The divergence angles and the transmitted optical power of LEDs for all cells are assumed to be the same. In this multi-cell configuration, depending on the locations of the mobile users (MUs), it would be advantageous to set all other unused transmitters into off mode, which means the LEDs are only used for lighting only, and no signal are modulated and transmitted. Therefore, the unnecessary ISI caused by the by neighbour transmitters are avoided.

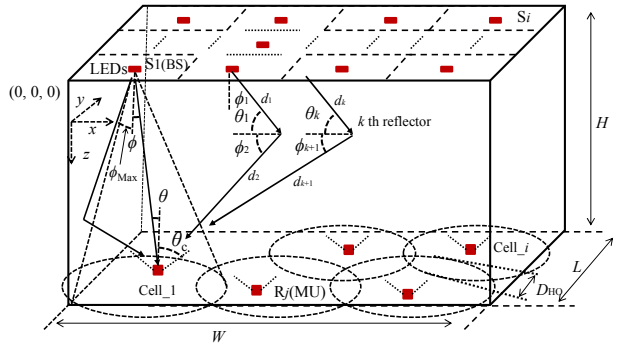

Fig. 1. An indoor OWC link with a multi-cell configuration.

B. OWC channel model with Lambertian sources

The indoor cellular OWC channel with the configuration is shown in Fig. 1. The radiation is emitted from a particular source S_i to a MU (R_j) with a location of (x, y, z). The incident radiations consist of directly unobstructed LOS paths and a finite number of k reflections from walls, ceiling and floor within the room. Assuming that the source S_i emits a unit impulse at $t = 0$ and normalizing the transmitted optical power P_{Tx} to 1. The LOS ($k = 0$) impulse response is given by [16]:

$$h^0(t; S_i, R_j) = \frac{(m+1)A}{2\pi d^2}\cos^m(\phi)T_s(\theta)g(\theta)\cos(\theta)\mathrm{rect}(\frac{\theta}{\theta_c})\delta(t-\frac{d_0}{c}), \quad (1)$$

where A is the photodetector surface area, θ_c is the FOV (semiangle) at the receiver. $T_S(\theta)$ is the optical filter gain, and $g(\theta)$ is the optical concentrator gain. d is the LOS distance between S_i and R_j, c is the speed of light and $\delta(.)$ is the Dirac delta function. The rectangular function rect(x) is defined as:

$$\mathrm{rect}(x) = \begin{cases} 1 & \text{for } |x| \le 1, \\ 0 & \text{for } |x| > 1. \end{cases} \quad (2)$$

Assuming that all reflectors are approximately Lambertian [21], the channel impulse response with multiple optical sources and multiple reflections is [22]:

$$h(t;\, S_i, R_j) = \sum_{n=1}^{N_{\text{source}}}\sum_{k=0}^{\infty} h_n^k(t;\, S_i, R_j) \quad (3)$$

The channel impulse response for k-bounce is given by [23]:

$$h^k(t;\, S, D) = \int_{\Psi}\left[\xi_0\xi_1 \dots \xi_k \rho^k\, \mathrm{rect}(\frac{\theta_k}{\theta_c}) \times \delta\left(t - \left(\frac{\sum_{k=0}^{\infty} d_k}{c}\right)\right)\right] dA_{\text{ref}}\ ,\ k \ge 1 \quad (4)$$

where

$$\xi_0 = \frac{(m+1)A}{2\pi d_1^2}\cos^m(\phi_1)\cos(\theta_1)\, dA_{ref}\cos\theta_1$$

$$\xi_1 = \frac{dA_{ref}\cos\phi_2\cos\theta_2}{\pi d_2^2}$$

, … ,

$$\xi_k = \frac{A\cos\phi_{k+1}\cos\theta_{k+1}}{\pi d_{k+1}^2} T_s(\theta_{k+1})g(\theta_{k+1}).$$

The integration in (4) is performed with respect to the surface of all reflectors, which is defined as Ψ. dA_{ref} is being the small area of the reflecting element, and ϕ_k and θ_k are the angles of irradiance and incidence, respectively. Also d_k is the distance from k bounces to the detector
The RMS delay spread is given by [14]:

$$S = \left[\frac{\int (t-\mu)^2 h^2(t)dt}{\int h^2(t)dt}\right]^{\frac{1}{2}}, \tag{5}$$

where μ is the mean delay given by:

$$\mu = \frac{\int t\, h^2(t)dt}{\int h^2(t)dt}. \tag{6}$$

and t is the propagation delay time.

III. Optimization Schemes

To achieve an optimal transmission bandwidth of the proposed cellular indoor OWC link, two optimization schemes are combined and adopted into the system. The details of these methods are introduced as following:

A. Optimal Divergence angles of LEDs

For an OWC link with a cellular configuration in Fig.1, due to the different multipath propagation delays, the ISI would limit the transmission bandwidth. To overcome this problem and to achieve a higher transmission bandwidth, the divergence angle of the LED can be tuned to its optimal value so that the ISI caused from neighbour cells and reflectors can be minimized. For each cell shown in Fig.1, the received optical power is maximum at $\phi = 0$ and minimum at $\phi = \phi_{\mathrm{Max}}$. The corresponding minimum received power which varies with m is:

$$P_{\mathrm{Min}} = P_{\mathrm{Tx}} \frac{(m+1)A}{2\pi {d_{\mathrm{Max}}}^2} \cos^m(\phi_{\mathrm{Max}}) T_s(\theta) g(\theta) \cos(\theta), \quad 0 \le \theta \le \theta_c, \tag{7}$$

where ϕ_{Max} is the maximum irradiance angle and d_{Max} is the corresponding maximum distance between the transmitter and the receiver within a cell. To increase P_{Min}, it is necessary to maximise P_{Min} for a given m. To do this, we calculate the partial derivation of (7) with respect to m, which is given by:

$$\frac{\partial P_{\mathrm{Min}}}{\partial m} = P_{\mathrm{Tx}}\, T_s(\theta) g(\theta) \cos(\theta) \frac{A}{2\pi {d_{\mathrm{Max}}}^2} \cos^m(\phi_{\mathrm{Max}}) \times \left\{1 + (m+1)\ln\left(\cos(\phi_{\mathrm{Max}})\right)\right\}. \tag{8}$$

Defining $K = P_{\mathrm{Tx}}\, T_s(\theta) g(\theta) \cos(\theta) \frac{A}{2\pi {d_{\mathrm{Max}}}^2}$, which is independent of m, (8) can be simplified to:

$$\frac{\partial P_{\mathrm{Min}}}{\partial m} = K \cos^m(\phi_{\mathrm{Max}}) \left\{1 + (m+1)\ln\left(\cos(\phi_{\mathrm{Max}})\right)\right\}. \tag{9}$$

To find the OLO m_{opt}, we set $\frac{\partial P_{\mathrm{Min}}}{\partial m} = 0$, which gives:

$$m_{\mathrm{opt}} = \frac{-1}{\ln\left(\cos(\phi_{\mathrm{Max}})\right)} - 1, \tag{10}$$

Given the definition of ϕ_{Max} above, we have:

$$\phi_{\mathrm{Max}} = \cos^{-1}\left(\frac{H}{d_{\mathrm{Max}}}\right). \tag{11}$$

$m = -\frac{\ln 2}{\ln(\cos\theta_{1/2})}$ is the Lambertian radiant order relating to the transmitter semiangle $\theta_{1/2}$, (at half power). The optimal transmitter semiangle $\theta_{1/2\,\mathrm{opt}}$ at half power can be calculated, which is given by:

$$\theta_{1/2\,\mathrm{opt}} = \cos^{-1}\left(\exp\left(\frac{-\ln(2)}{\frac{-1}{\ln(\cos(\phi_{\mathrm{Max}}))} - 1}\right)\right), \quad 0 < \theta_{1/2\,\mathrm{opt}} < 90^o. \tag{12}$$

B. Handover algorithm

In Fig. 1, the entire room is covered by a number of cells which transmit the same data. However, in real scenarios, MUs are randomly moving around within and between cells. To minimize the ISI, cells could be switched into off mode when there are no active MUs within them. To achieve this, a handover process is adopted into the system and the flow chart for a single cell is shown in Fig. 2.

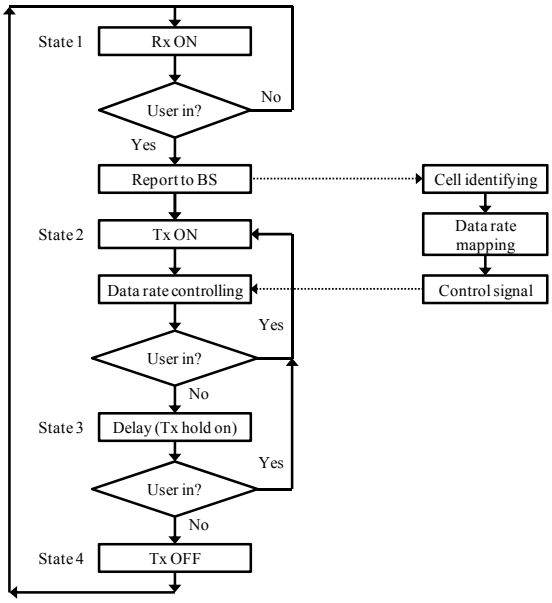

Fig. 2. Flow diagram for handover algorithm within each cell.

In state 1, the BS receiver (the transreceiver integrated with S_i at the ceiling) is on to detect the presence of a MU within a cell. The BS first identifies the address of the active cell and then establishes a link with the MU at a minimum predicted transmission data rate (see the state 2 in Fig. 2). Once the link has been established, the BS will count the number of the active cells within the room and then map the corresponding maximum transmission data rate for this link. Following this a control signal is sent back to each cell to adaptive the data rate to its maximum value. If BS fails to receive an active signal from MU within a cell, the corresponding BS is switched to the off mode. In real scenarios, the MU located in overlapping area could be in communication with two BSs. To maximize the handover efficiency and to avoid too many handovers, the BS will continue to provide the coverage for a short time in order to confirm the absence of MU. By double checking to ensure that there is no signal, the BS will be switched to the off mode state, as illustrated by states 2 to 4 in Fig. 2.

The duration between states 1 and 2 is equal to T_{ho}, which is defined as the handover time.

$$T_{\mathrm{ho}} < \frac{D_{\mathrm{HO}}}{V_{\mathrm{MU}}} \tag{13}$$

where D_{HO} is the horizontal overlap distance, and V_{MU} is the typical speed of the MU.

In [24, 25], it has been reported that the typical speed of human is less than 3 m/s ($V_{\mathrm{MU}} < 3\ \mathrm{m/s}$). That means for a horizontal overlap distance $D_{\mathrm{HO}} = 0.1$ m, the corresponding T_{ho} should be less than ~ 0.03 second. When MU is located within the overlapping area, the MU could be at an equal distance from two BSs. In this case, due to the equal distance, the multipath induced ISI is very low (it will be shown in the following Section IV). Therefore, two BSs are active until the MU moves into one of cell.

IV. Results and Discussions

In order to carry out a comparative study of the proposed system employing different optimization techniques, the OWC channel characteristics are simulated. In this simulation, the computational time for determining the impulse response is limited to two bounces $k = 2$ and the bin width of impulse response is defined as $\Delta t = 0.1$ ns, which are the same as in [26]. The specifications and the parameters are given in Table 1. From (10) and (12), the optimum divergence angle of the four-cell configuration can be calculated, which is 56° at FWHM. In this paper, only four-cell configuration is simulated and presented. However, the two optimization techniques introduced in Section III could also be adopted in other cellular configurations.

A. Power distribuion with and without OLO

Fig. 4 (a) and (b) compare the received optical power distributions of a four-cell configuration with and without the

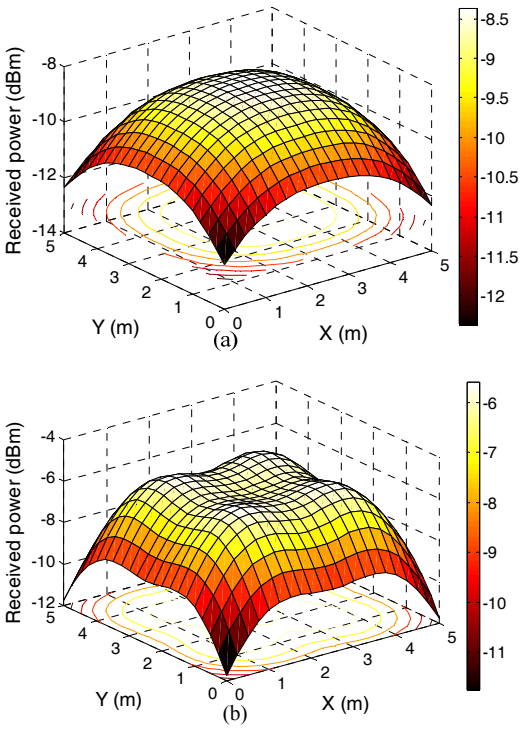

Fig. 3. Spatial distribution of received power: (a) four-cell configuration with 120° FWHM angle, and (b) four-cell with 56° FWHM angle.

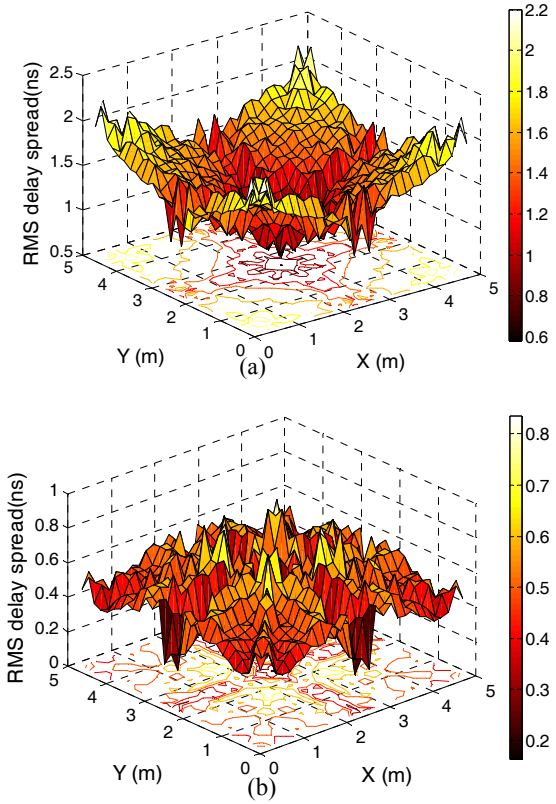

Fig. 4. Spatial distribution of RMS delay spread: (a) four-cell configuration with 120° FWHM angle, and (b) four-cell with 56° FWHM angle.

TABLEI: SPECIFICATION FOR CELLULAR INDOOR OWC SYSTEMS

LED wavelength (λ)	(500~1000) nm
LED launched power	200 mW
LED spacing	0.05 m
Room (length, width, height)	$5 \times 5 \times 3$ m^3
Half angle FOV of receiver	60 (deg)
Active area of photodiode	16 mm^2
Gain of the optical filter	1.0
Reflection coefficient (wall, ceiling, floor)	(0.8, 0.8, 0.3)
Number of LEDs per cell	36
Cell size	2.5×2.5 m^2

optimal divergence angle. The received optical power varies between -8.4 dBm and -12.4 dBm for non-optimized angle (m=1, 120^o FWHM) and between -5.6 dBm and -11.7 dBm for optimized angle (m= OLO, 56^o FWHM). In this case, angle optimization allows 0.7 dB and 2.8 dB increase for minimum and maximum received powers, respectively.

B. RMS delay spread with OLO.

To investigate the channel transmission bandwidth, the channel dispersion for the described case studies in Table 1 will be characterized. Figs. 4(a) and (b) show the RMS delay spreads of the four-cell configurations with and without OLO. By tuning the divergence angle to its optimal value, it is observed that a significant reduction of the mean RMS, which is decreased from ~ 1.5 ns to ~ 0.4 ns. In addition, the multipath distortion at the room corners is quite significant because it limits the transmission bandwidth of the system. In Fig. 4, it also can be seen that the RMS delay spreads at the room corners have a significant reduction as well. From ~ 2ns to ~ 0.8 for non-optimization and optimization cases respectively.

C. RMS delay spread with a handover algorithm

Fig. 5(a) shows the contour plot of the RMS delay spread distribution. The near square area highlighted on the *x-y* axes is the location range for MUs. It illustrates that the maximum D_{rms} within the coverage area of the active BS is ~0.2 ns, thus offering a maximum transmission rate of 500 Mbit/s. Note that the maximum achievable data rate without any equalization is $R_{\text{b}} \leq \left(10D_{\text{rms\_Max}}\right)^{-1}$ [27]. If all MUs are located within two adjacent cells or in the overlapping areas between cells except the center of the room (see Fig. 4(b)), the simulated RMS delay spread for this case is depicted in Fig. 5(b). For this case, the maximum D_{rms} ~0.4 ns, which corresponds to almost half the maximum achievable data rate of previous case. Similarly, the simulated RMS delay spread for three active cells is depicted in Fig. 5(c). The maximum RMS delay spread within coverage areas of active BSs is around ~ 1ns, which corresponds to the maximum achievable data rate of ~ 100 Mbit/s. This is the worst case, where the number of MUs within cells is high or MUs are moving around randomly within all four cells so that all BSs are in the active mode. The simulated RMS delay spread distribution for this case outlined in Fig. 5(d). The delay spread is the highest with a maximum value of ~ 1.2 ns. Hence, the maximum

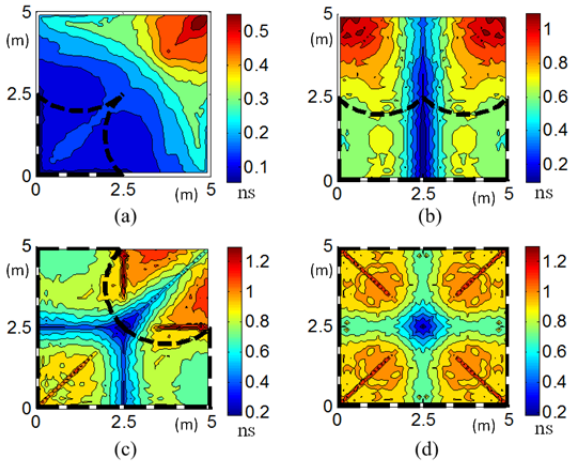

Fig. 5. The contour plot of RMS delay spreads of a four-cell OWC system: (a) 1 BS actives, (b) 2 BSs active, (c) 3 BSs active and (d) 4 BSs active.

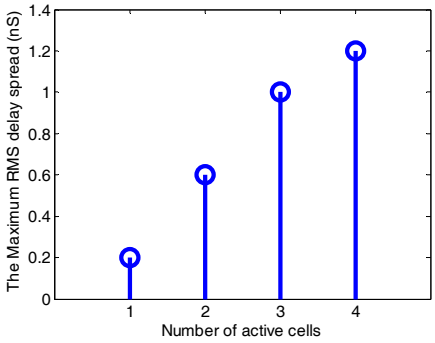

Fig. 6. The maximum RMS delay spread of four different cases.

achievable data rate is ~83 Mbit/s. The maximum RMS delay spreads for different cases from one to four active cells are plotted in Fig. 6. It can be seen the RMS delay spread increases with the active BSs. This is due to increased number of multipath propagation paths, which will limit the achievable maximum data rate. This problem can be overcome by using a cell with a small coverage area. However this will lead to increase in number of transceivers and therefore more handovers, thus leading to increased overall system complexity. Therefore, the numbers of cells and sizes of the footprints are quite critical for the maximum transmission bandwidth, which need to be carefully taken into account when designing an indoor OWC system.

CONCLUSION

In this paper, a cellular indoor OWC system is studied. Two optimization techniques are proposed to increase the transmission bandwidth of the system. The results showed that there was a significant improvement in the improved received optical power as well as the multipath induced distortion by using OLO. By adopting a handover algorithm in to the system, the transmission bandwidth could be further extended. The simulation results showed that with applying the handover algorithm, the maximum transmission data rate for the best scenario (only one cell in active mode the divergence angle of the LED is 56^o FWHM) can be

improved more than ten times comparing with the worst case (All cells are in active mode and the divergence angle of the LED is 120^o FWHM).

AKNOWLEDGMENT

This work is support by the EU COST Action IC1101.

REFERENCES

[1] N. Ghazisaidi, M. Maier, and C. M. Assi, "Fiber-wireless (FiWi) access networks: A survey," *Communications Magazine, IEEE,* vol. 47, pp. 160-167, 2009.

[2] C. B. Nelson, B. D. Steckler, and J. A. Stamberger, "The Evolution of Hastily Formed Networks for Disaster Response: Technologies, Case Studies, and Future Trends," in *Global Humanitarian Technology Conference (GHTC), 2011 IEEE*, 2011, pp. 467-475.

[3] M. Sherman, A. N. Mody, R. Martinez, C. Rodriguez, and R. Reddy, "IEEE Standards Supporting Cognitive Radio and Networks, Dynamic Spectrum Access, and Coexistence," *Communications Magazine, IEEE,* vol. 46, pp. 72-79, 2008.

[4] D. Aguayo, J. Bicket, S. Biswas, G. Judd, and R. Morris, "Link-level measurements from an 802.11b mesh network," *Computer Communication Review,* vol. 34, pp. 121-131, Oct 2004.

[5] "IEEE Standard for Information technology-- Local and metropolitan area networks-- Specific requirements-- Part 11: Wireless LAN Medium Access Control (MAC)and Physical Layer (PHY) Specifications Amendment 5: Enhancements for Higher Throughput," *IEEE Std 802.11n-2009 (Amendment to IEEE Std 802.11-2007 as amended by IEEE Std 802.11k-2008, IEEE Std 802.11r-2008, IEEE Std 802.11y-2008, and IEEE Std 802.11w-2009),* pp. 1-565, 2009.

[6] Z. Ghassemlooy, W. Popoola, and S. Rajbhandari, *Optical wireless communication: system and channel modeling with MATLAB*. Newcastle upon Tyne: CRC Press, 2012.

[7] Y. Tanaka, T. Komine, S. Haruyama, and M. Nakagawa, "A basic study of optical OFDM system for indoor visible communication utilizing plural white LEDs as lighting," *Proceeding of 8th International Symposium on Microwave and Optical Technology (ISMOT),* pp. 303-306, 2001.

[8] J. P. Conti, "What you see is what you send - [comms visible light]," *Engineering & Technology,* vol. 3, pp. 66-69, 2008.

[9] *Safety of laser products - Part 1: Equipment classification and requirements*, 2007.

[10] J. Grubor, S. Randel, K. D. Langer, and J. W. Walewski, "Broadband Information Broadcasting Using LED-Based Interior Lighting," *Lightwave Technology, Journal of,* vol. 26, pp. 3883-3892, 2008.

[11] D. Tsonev, C. Hyunchae, S. Rajbhandari, J. J. D. McKendry, S. Videv, E. Gu*, et al.*, "A 3-Gb/s Single-LED OFDM-Based Wireless VLC Link Using a Gallium Nitride μLED," *Photonics Technology Letters, IEEE,* vol. 26, pp. 637-640, 2014.

[12] J. R. Barry, J. M. Kahn, W. J. Krause, E. A. Lee, and D. G. Messerschmitt, "Simulation of multipath impulse response for indoor wireless optical channels," *IEEE Journal on Selected Areas in Communications,* vol. 11, pp. 367 - 379, 1993.

[13] J. B. Carruthers and J. M. Kahn, "Modeling of nondirected wireless Infrared channels," *IEEE Transaction on Communication,* vol. 45, pp. 1260-1268, 1997.

[14] J. B. Carruthers, S. M. Caroll, and P. Kannan, "Propagation modelling for indoor optical wireless communications using fast multi-receiver channel estimation," *IEE Proceedings-Optoelectronics,* vol. 150, pp. 473-481, 2003.

[15] D. Wu, Z. Ghassemlooy, H. Le Minh, S. Rajbhandari, and M. A. Khalighi, "Optimisation of Lambertian order for indoor non-directed optical wireless communication," in *Communications in China Workshops (ICCC), 2012 1st IEEE International Conference on*, 2012, pp. 43-48.

[16] J. B. Carruthers and S. M. Carroll, "Statistical impulse response models for indoor optical wireless channels," *International Journal of Communication Systems,* vol. 18, pp. 267-284, 2005.

[17] J. B. Carruther and J. M. Kahn, "Angle diversity for nondirected wireless infrared communication," *Communications, IEEE Transactions on,* vol. 48, pp. 960-969, 2000.

[18] D. Wu, Z. Ghassemlooy, M. Hoa Le, S. Rajbhandari, and Y. S. Kavian, "Power distribution and q-factor analysis of diffuse cellular indoor visible light communication systems," presented at the European Conference on Networks and Optical Communications (NOC), Newcastle Upon Tyne UK, 2011.

[19] D. Wu, Z. Ghassemlooy, M. Hoa Le, S. Rajbhandari, and C. Lu, "Channel characteristics analysis of diffuse indoor cellular optical wireless communication systems," *Proc. of SPIE,* vol. 8309, 2011.

[20] T. Borogovac, M. Rahaim, and J. B. Carruthers, "Spotlighting for visible light communications and illumination," in *GLOBECOM Workshops (GC Wkshps), 2010 IEEE*, Miami, Florida, USA, 2010, pp. 1077-1081.

[21] J. M. Kahn and J. R. Barry, "Wireless infrared communications," *Proceedings of IEEE,* vol. 85, pp. 265-298, 1997.

[22] F. R. Gfeller and U. Bapst, "Wireless in-house data communication via diffuse infrared radiation," *Proceedings of the IEEE,* vol. 67, pp. 1474- 1486, 1979.

[23] L. Kwonhyung, P. Hyuncheol, and J. R. Barry, "Indoor channel characteristics for visible light communications," *IEEE Communications Letters,* vol. 15, pp. 217-219, 2011.

[24] A. Kotsopoulos and T. Antonakopoulos, "Modeling the dynamics of MEMS-based mobile devices under speed-controlled human motion using acceleration measurements," in *Instrumentation and Measurement Technology Conference, 2009. I2MTC '09. IEEE*, 2009, pp. 968-972.

[25] M. Vela Nunez, C. A. Avizzano, E. Ruffaldi, and M. Bergamasco, "A low-cost human locomotion speed recognition for augmented virtual environments exploration," in *Human System Interactions (HSI), 2011 4th International Conference on*, 2011, pp. 136-143.

[26] M. D. Higgins, R. J. Green, and M. S. Leeson, "A Genetic Algorithm Method for Optical Wireless Channel Control," *Lightwave Technology, Journal of,* vol. 27, pp. 760-772, 2009.

[27] T. S. Rappaport, *Wireless Communications*: Prentice-Hall, 2002.